REGULAR PAPER

J. Physiol. Sci. Vol. 57, No. 6; Dec. 2007; pp. 327–335
Online Nov. 6, 2007; **doi:10.2170/physiolsci.RP010107**

A Simple Technique for Isolating Healthy Heart Cells from Mouse Models

Takao SHIOYA
Department of Physiology, Faculty of Medicine, Saga University, Saga, 849-8501 Japan

Abstract: Single heart cells of mouse models provide powerful tools for heart research. However, their isolation is not easy, and it imposes a significant bottleneck on their use in cellular studies of the heart. Aiming to overcome this problem, this report introduces a novel technique that reproducibly isolates healthy heart cells from mouse models. Using simple devices that ensure easy handling and the rapid aortic cannulation of a small mouse heart, cell isolation was done under physiological conditions without using the "KB" medium or 2,3-butanedione monoxime (BDM). The isolated cells consistently had a healthy appearance and a high viability of 75 ± 5% (mean ± SD) in Tyrode solution containing 1.8 mM Ca^{2+}. After 8 h of storage at 37°C, they still had a viability of 45 ± 12%. The cells showed normal contraction properties when field-stimulated, and they generated normal action potentials and membrane currents under the whole-cell clamp condition. The β-adrenergic signal transduction of the cells was also normal when it was examined with the isoproterenol enhancement of the L-type Ca^{2+} current.

Key words: mouse, cardiac myocyte, contraction, action potential, ionic current.

Single heart cells of mouse models provide powerful tools for heart research. In these cells, one can take advantage of the versatility of recent genetic engineering technology [1] and also of the accuracy of single-cell measurement techniques such as patch-clamp and Ca^{2+} imaging. So far, molecular mechanisms of fundamental heart functions, such as excitation-contraction coupling, action potential shaping, and β-adrenergic signaling, have been successfully unveiled by using single heart cells of mouse models [2–7]. Moreover, these cells also provide a convenient platform for analyzing pathogenic mechanisms and the pathophysiology of hereditary heart diseases in molecular detail [8, 9].

For such single-cell studies, healthy heart cells are absolutely necessary; however, their isolation from mouse models is not easy. Surgery and aortic cannulation of a small mouse heart are hard to do and require a long time, and during that time, the heart suffers from complete ischemia. Consequently, the cells isolated from these hearts show various signs of ischemic damages, such as bizarre appearance, low viability levels, and abnormalities in their excitation and contraction properties. Cells of these kinds are hard to use for the experiment, and the data they provide are often difficult to interpret. This issue imposes a significant bottleneck on the use of mouse heart cells and is especially problematic in genetically engineered mouse models that are usually available only in limited amounts.

To solve this problem, two major work-arounds have been devised and used for heart cell isolation from mouse models. One is to incubate the cells in high-K^+, Ca^{2+}-free "KB" medium at 4°C [10, 11], and the other is to administer 10–20 mM 2,3-butanedione monoxime (BDM) in the media for cell isolation and storage [12, 13]. Both work-arounds proved to be highly effective for reducing ischemic damages to the cells [12, 14]; however, they need to expose the cells to nonphysiological environments that reportedly affect the cells' physiological properties [14–17]. To conserve the physiology of the cells *in vivo*, cell isolation under physiological conditions is more desirable.

This report introduces a novel technique that reproducibly isolates healthy heart cells from mouse models under physiological conditions. Instead of using work-arounds, this technique uses simple devices that help the surgery and aortic cannulation of the heart to prevent the development of ischemic damages. The isolated heart cells had a high viability, a long storage life, and normal excitation and contraction properties. Part of this work has previously appeared in abstract form [18].

Received on Sep 11, 2007; accepted on Nov 2, 2007; released online on Nov 6, 2007; doi:10.2170/physiolsci.RP010107
Correspondence should be addressed to: T. Shioya, Department of Physiology, Faculty of Medicine, Saga University, 5-1-1 Nabeshima, Saga 849-8501, Japan. Phone: +81 952-34-2274, Fax: +81 952-34-2013, E-mail: shioya@cc.saga-u.ac.jp

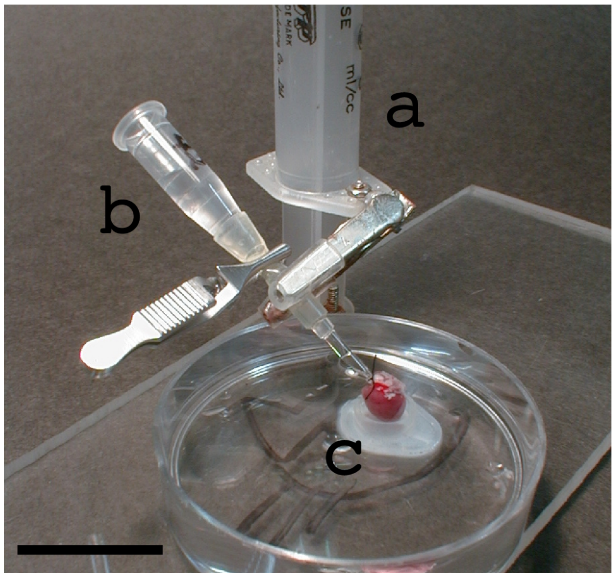

Fig. 1. The cannulation device. The cannula holder (**a**) kept the aortic cannula (**b**) at a ~30° angle at variable height. The heart was held upright in the bath (**c**), which was a plastic dish (60-mm diameter × 13-mm height) with a heart stand (lid of 1.5 ml Eppendorf tube) glued on the bottom. The cannula holder was composed of a Perspex base plate (190 × 70 × 5 mm), a 5-ml syringe with its plunger glued to the base plate, and a small alligator clip attached to the syringe barrel. The gasket (tip rubber) of the syringe plunger was glued to the plunger rod to eliminate horizontal play in the cannula's position. The jaws of the alligator clip were covered with silicone tubing to ensure a firm grip. The bulldog clamp was used to pinch the cannula at its silicone tubing joint to retain the solution in the cannula. Scale: 20 mm.

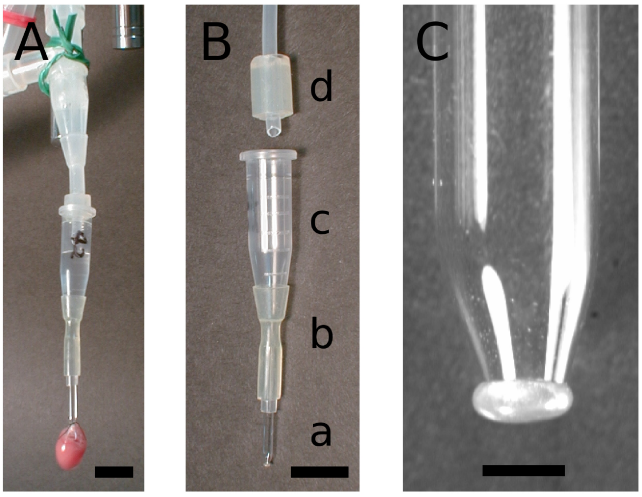

Fig. 2. The aortic cannula. (**A**) The heart was connected to the water-jacketed perfusion line (dead volume 4.5 ml) via the aortic cannula, which was designed to function also as an air trap. Scale: 10 mm. (**B**) The cannula was composed of a glass shaft (**a**), a shaft-reservoir joint made of silicone tubing (**b**), and a solution reservoir that was a 0.5-ml Eppendorf tube with its lid and bottom trimmed off (**c**). The perfusion line was 2.7-mm diameter polyethylene tubing (#8, Hibiki, Tokyo, Japan), and had a silicone plug at its end (**d**) so that it could make an airtight fit into the reservoir. Scale: 10 mm. (**C**) The shaft was fabricated from 2-mm diameter glass capillary (#14-084-13, Hilgenberg), using a vertical puller (PP-83, Narishige). Under the dissection microscope, its tip was sanded down to 0.6–0.8 mm diameter, using fine-grid (#800) sandpaper, and the tip bulge was created with 5 min curing epoxy glue (e.g., Araldite Rapid). To do this, a small amount of the glue about to cure was picked up with a toothpick and wrapped around the cannula's tip by rotating the cannula shaft. The outer diameter of the tip bulge *d* (mm) suitable for a mouse having *w* (g) body weight was approximated as $d = 0.6 + 0.015w$. Scale: 1 mm.

MATERIALS AND METHODS

Isolation of single heart cells. Heart cells were isolated from adult C57BL/6J mice (6–12 weeks old; Clea Japan, Tokyo, Japan). Procedures for the handling and care of the mice fully conformed to Guiding Principles for the Care and Use of Animals in the Field of Physiological Sciences and were approved by the Saga University Animal Care and Use Committee.

A mouse was heparinized (8,000 U/kg, i.p.) and deeply anesthetized with an overdose of pentobarbital sodium (300 mg/kg, i.p.), then held in a dorsal position by taping its legs. Its upper abdomen was opened horizontally, and the ribs and sternum were removed to widely open the chest cavity. The exposed heart was held by suction in the tip (cut to ~5 mm diameter) of a 3.5-ml soft plastic transfer pipette (#86.1171, Sarstedt, Nümbrecht, Germany) and was quickly excised with the use of curved scissors (#14215, WPI, Sarasota FL, USA). The heart was immediately cooled and cleaned of debris in ice-cold cell isolation buffer supplemented with 0.4 mM EGTA (EGTA-CIB). Cell isolation buffer (CIB) contained (mM) 130 NaCl, 5.4 KCl, 0.5 $MgCl_2$, 0.33 NaH_2PO_4, 22 glucose, 50 μU/ml bovine insulin (I-5500, Sigma), and 25 HEPES-NaOH (pH = 7.4). Insulin was used from 1 U/ml stock solution in 0.1 mM HCl (pH = 4.0), and the EGTA was from 400 mM stock in 1 M NaOH (pH = 7.8).

The excised heart was cannulated through the aorta, using the cannulation device shown in Fig. 1. The heart was immersed in ice-cold EGTA-CIB in the bath, where it was held upright under the solution level. Before surgery, the aortic cannula (Fig. 2) was filled with EGTA-CIB, and a ~100 mm piece of 6-0 black silk suture was loosely tied on its shaft. The cannula was mounted on the cannulation device, and its tip was positioned under the solution level and right next to the aorta by adjusting the cannulation device. Under the dissection microscope, the aorta was put over the cannula's tip, using two fine forceps (#5, Dumont, Switzerland); it was then secured to the cannula by using the suture tied on the shaft. In this way, the aortic cannulation of a small mouse heart could be done easily

and rapidly, without risk of air embolism. The total time for surgery and aortic cannulation was usually less than 5 min.

The cannulated heart was then connected to a water-jacketed perfusion line, as shown in Fig. 2A. The heart was retrogradely perfused at a constant hydrostatic pressure of 70-cm H_2O at 37°C, initially with EGTA-CIB, for 3–4 min. During this period, the interventricular septum was incised to facilitate heart perfusion because a fast flow rate was vital for isolating healthy cells. To do this, the atria were partially removed with small scissors (#14088-10, FST, Foster City, CA, USA) to make access holes to the ventricular cavities, and the scissors' blades were inserted into these holes to incise the septum in between. The flow rate of perfusion at this stage, which was measured by counting perfusate drops falling off the heart, was 8–10 drops/10 s. Oxygen bubbling of the perfusate made no obvious difference to the condition of the isolated cells and was not used in this technique.

The perfusate was then switched to the enzyme solution (15 ml), which was CIB supplemented with 0.3 mM $CaCl_2$, 1 mg/ml collagenase (CLS-2, Worthington Biochemical, Lakewood, NJ, USA), 0.06 mg/ml trypsin (T-8003, Sigma, St. Louis, MO, USA), and 0.06 mg/ml protease (P-5147, Sigma). Once the switch to this solution was made, the flow rate temporarily dropped 30–50% for 1–2 min. The solution was recirculated for 6–9 min after discarding the initial ~5 ml fraction until the flow rate reached twice the initial level, or 20 drops/10 s.

From the digested heart, the ventricles were excised and shredded into several pieces. The tissue pieces were then further digested in fresh enzyme solution (15 ml) for 15–20 min at 37°C until they were almost completely dissociated. In this enzyme solution, the $CaCl_2$ level was increased to 0.7 mM, and 2 mg/ml BSA (A-9418, Sigma) was supplemented. Gentle stirring facilitated dissociation of the tissue; however, caution must be used because excess mechanical agitation will cause damage to the cells.

The cell suspension was centrifuged in a 15-ml plastic conical tube at 14 × *g* (300 rpm) for 3 min. The cell pellet (~0.1 ml) was resuspended in 15 ml CIB supplemented with 1.2 mM $CaCl_2$ and 2 mg/ml BSA. The cells were incubated at 37°C for 10 min, centrifuged (14 × *g*, 3 min), and then resuspended in 10 ml Tyrode solution supplemented with 2 mg/ml BSA, 1× penicillin/streptomycin (P-4458, Sigma), and 15 μg/ml phenol red for pH monitor. The Tyrode solution contained (mM) 140 NaCl, 5.4 KCl, 1.8 $CaCl_2$, 0.5 $MgCl_2$, 0.33 NaH_2PO_4, 11 glucose, and 5 HEPES-NaOH (pH = 7.4). The isolated cells were stored at 37°C in 15-ml plastic tubes, which were laid flat for better oxygen supply.

The total time required for the above procedures was ~70 min. After every cell isolation, the perfusion line was cleaned with 1 M NaOH (locked in the line for an hour) and was thoroughly rinsed with plenty of distilled water.

Electrophysiology. Action potentials and macroscopic membrane current were recorded under the whole-cell clamp condition. The cells were current- or voltage-clamped, using a custom-built patch-clamp amplifier, while they were superfused with Tyrode solution at 37°C. The patch pipettes were fabricated from 1.5-mm diameter thin-walled glass capillaries (#14-082-13, Hilgenberg, Malsfeld, Germany), using a vertical puller (PP-83, Narishige, Tokyo, Japan), and had a 2–4 MΩ resistance when filled. The pipette solution contained (mM) 110 K-aspartate, 30 KCl, 10 NaCl, 5 Mg-ATP, 1 EGTA, 0.1 Tris-GTP, and 20 HEPES-KOH (pH = 7.2).

To record the L-type Ca^{2+} current, a separate set of solutions was used. Cs^+-pipette solution contained (mM) 110 Cs-aspartate, 30 CsCl, 5 Mg-ATP, 5 TEA-Cl, 1 EGTA, 0.1 Tris-GTP, and 20 HEPES-CsOH (pH = 7.2). Cs^+-Tyrode solution contained (mM) 140 NaCl, 5.4 CsCl, 1.8 $CaCl_2$, 0.5 $MgCl_2$, 0.33 NaH_2PO_4, 3 4-AP, 11 glucose, and 5 HEPES-NaOH (pH = 7.4).

The acquisition and analysis of electrophysiological data were done on a PC, using pClamp 8 software suite (Axon, Foster City, CA, USA) and signal interface hardware (DigiData 1200, Axon) at a sampling frequency of 20 kHz. Current pulses for field stimulation and for evoking action potentials under current clamp were generated by using an electronic stimulator (SEN-3203, Nihon Koden, Tokyo, Japan). A liquid junction potential of –8.1 ± 1.1 mV (n = 10) was observed between the pipette solution and the Tyrode solution. All voltage data in this report were corrected according to this value.

Measurement of single-cell contraction. Unloaded contractions of the cells were monitored with a CCD video camera (CS-3330, Teli, Tokyo, Japan) mounted on the side port of an inverted microscope (TMD-300, Nikon, Tokyo, Japan). The video signal was digitized online into TIFF files, using Scion Image software (Scion, Frederick MD, USA), on a PC with a frame-grabber card (LG-3, Scion). The TIFF files were analyzed offline by using a custom macro program written for Scion Image that measures the waveform of cell shortening by tracking the cell edges at a time resolution of 16.7 ms. This video system was also used for measuring the cells' dimensions and sarcomere length.

Statistics. Data values were expressed as mean ± SD (n = number of cells for single-cell measurements or number of preparations for others). The statistical difference between means was examined with Student's t-test, and significance was assumed when $p < 0.05$. For multiple comparisons, one-way ANOVA was used instead.

RESULTS

Appearance of the cells

Pictures of the mouse heart cells prepared as described above are shown in Fig. 3A. In Tyrode solution containing

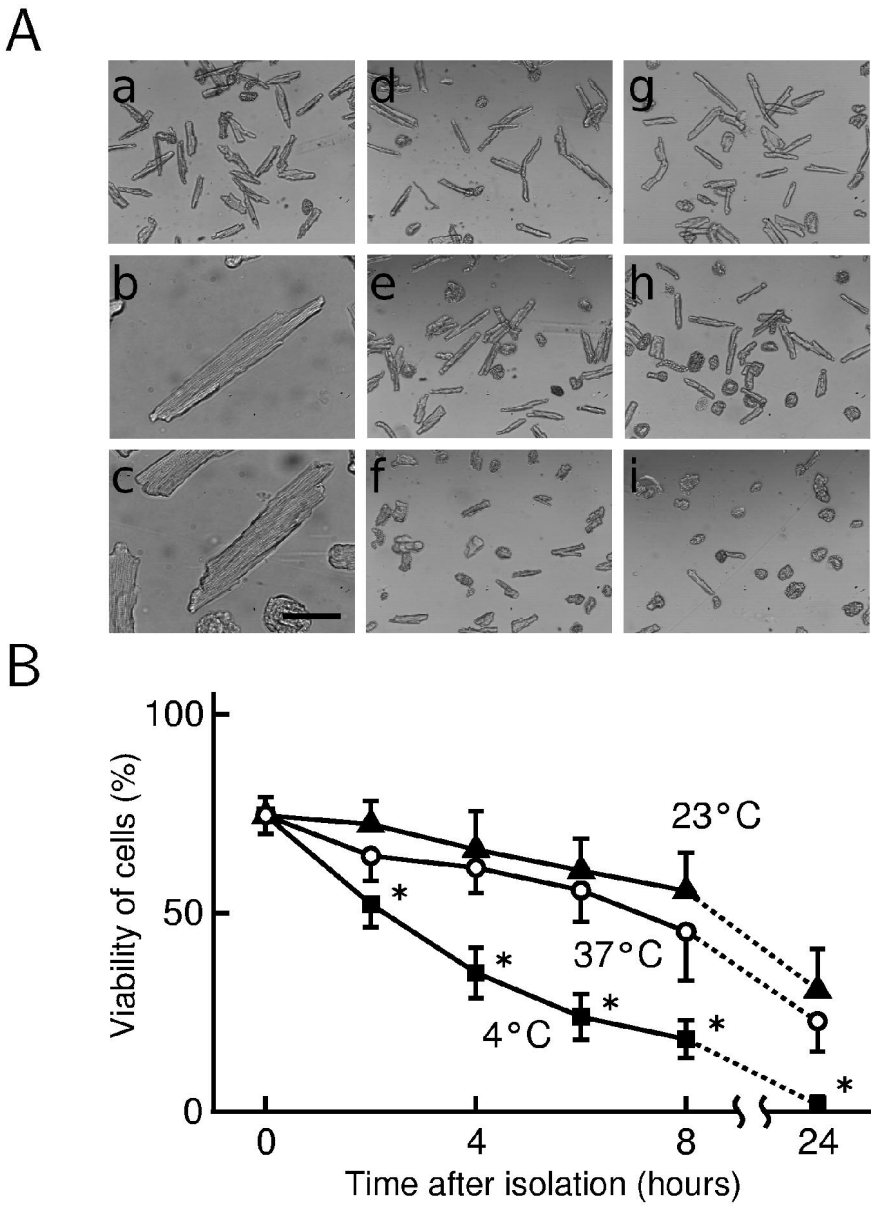

Fig. 3. Appearance and storage life of the cells in Tyrode solution. (**A**) Left column: the cells at the time of isolation at 10× (**a**) and 40× (**b**) magnifications, and those stored for 8 hours at 37°C at 40× (**c**). Center and right columns: the cells stored for 4 (center) or 8 hours (right) at 37 (**d**, **g**), 23 (**e**, **h**), or 4°C (**f**, **i**) at 10×. Scale: 160 (10×) or 40 μm (40×). (**B**) Time course of the cells' viability during storage at 37 (open circles), 23 (solid triangles), or 4°C (solid squares). Error bars indicate SD (n = 5). Asterisks indicate significant difference ($p < 0.05$) from the value at 37°C.

1.8 mM Ca^{2+}, the cells were relaxed and rod shaped with clear striations of sarcomeres. Viability of the cells, which was defined as the percentage of relaxed and rod-shaped cells in total cell count, was 75 ± 5% (n = 5) at the time of cell isolation. This high viability level with a small SD indicates a consistent yield of healthy heart cells. The length and the width of the cells were 157 ± 23 and 25 ± 5 μm (n = 38), respectively, and their sarcomere length was 1.88 ± 0.05 μm (n = 38). Their membrane capacitance, which was measured from the capacitive current in voltage-clamp experiments, was 151 ± 27 pF (n = 35). These values are in good agreement with the values reported for mouse heart cells [10, 19, 20].

Storage life of the cells

The storage life of the cells was examined in Fig. 3. The cells suspended in Tyrode solution (supplemented as described above) were divided into three equal aliquots at the time of cell isolation, and each aliquot was stored at 37, 23, or 4°C. At 37 and 23°C, the cells showed no obvious change in their appearance after 8 h of storage (Fig. 3A), although their viability levels decreased to 45 ± 12% (n = 5) at 37°C, or to 56 ± 10% (n = 5) at 23°C (Fig. 3B). After 24 h of storage, the cells still maintained a viability level of 23 ± 8% (n = 5) at 37°C, and 31 ± 10% (n = 5) at 23°C. This result indicates that the cells have a long storage life, enough to be used as an acutely isolated heart cell preparation.

In contrast, the cells stored at 4°C developed obvious cell shortening and membrane blebs (Fig. 3A). Their viability level after 8 h of storage (Fig. 3B) was only 18 ± 5% (n = 5), and after 24 h almost no cells were surviving (2 ± 2%, n = 5). This poor cell preservation at 4°C would be attributed to strong metabolic inhibition at this low temperature.

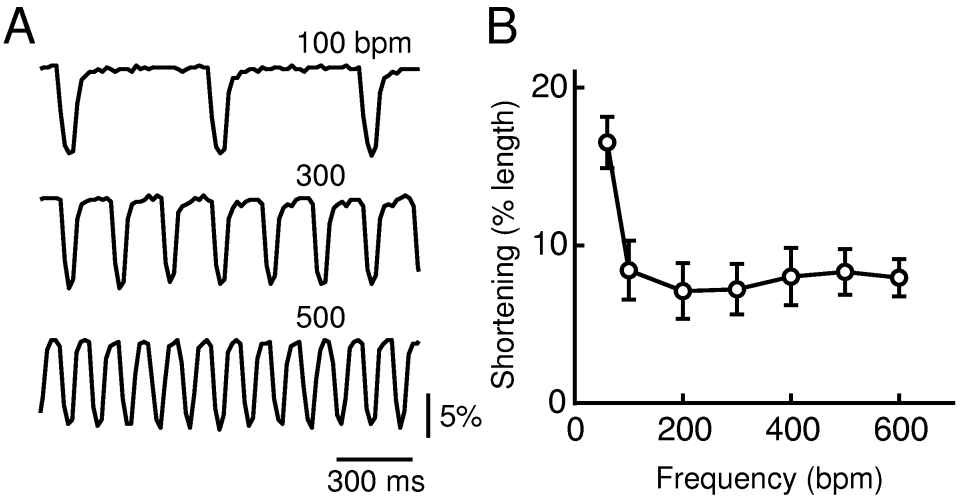

Fig. 4. Unloaded contraction of the cells. (**A**) Waveforms of the unloaded contraction evoked by field stimulation at 100 (top), 300 (middle), and 500 bpm (bottom). Resting cell length was 141 μm. (**B**) Dependence of the contraction amplitude on the stimulation frequency. The values are expressed as the percentage to resting cell length. Error bars indicate SD (n = 8).

Contraction properties of the cells

In Fig. 4, contractions of the cells were measured in Tyrode solution at 37°C. The cells were field-stimulated with 2 ms suprathreshold current pulses at a frequency of 60–600 beats/min (bpm), or 1–10 Hz, which is close to the physiological heart rates of the mouse (180–650 bpm) [21]. Upon stimulation, the cells showed a rapid and large contraction, as illustrated in Fig. 4A. The contraction had an amplitude of 8.2 ± 2.2% (n = 8) of the resting cell length at a stimulation frequency of 300 bpm, and was larger at lower stimulation frequency (16.5 ± 1.6% at 60 bpm), being consistent with the negative force-frequency relation known for the heart muscle of the mouse [17, 19, 22, 23]. However, in the range of physiological heart rates (200–600 bpm), the contraction amplitude showed no significant frequency-dependence (p = 0.47 by one-way ANOVA).

Action potentials of the cells

The action potentials of the cells were recorded under the whole-cell clamp condition in Fig. 5. Establishing gigaseal and break-in was trivial in these cells. The cells had a resting membrane potential of –75.0 ± 2.1 mV (n = 14) when current-clamped in Tyrode solution at 37°C. Figure 5A shows the action potentials of the cells, which were evoked by injecting 2-ms suprathreshold current pulses via the patch pipette. The action potentials were brief and had a spike-and-tail waveform as was reported for mouse heart cells [11, 24]. Under this experimental condition, the action potentials initiated no detectable cell shortening be-

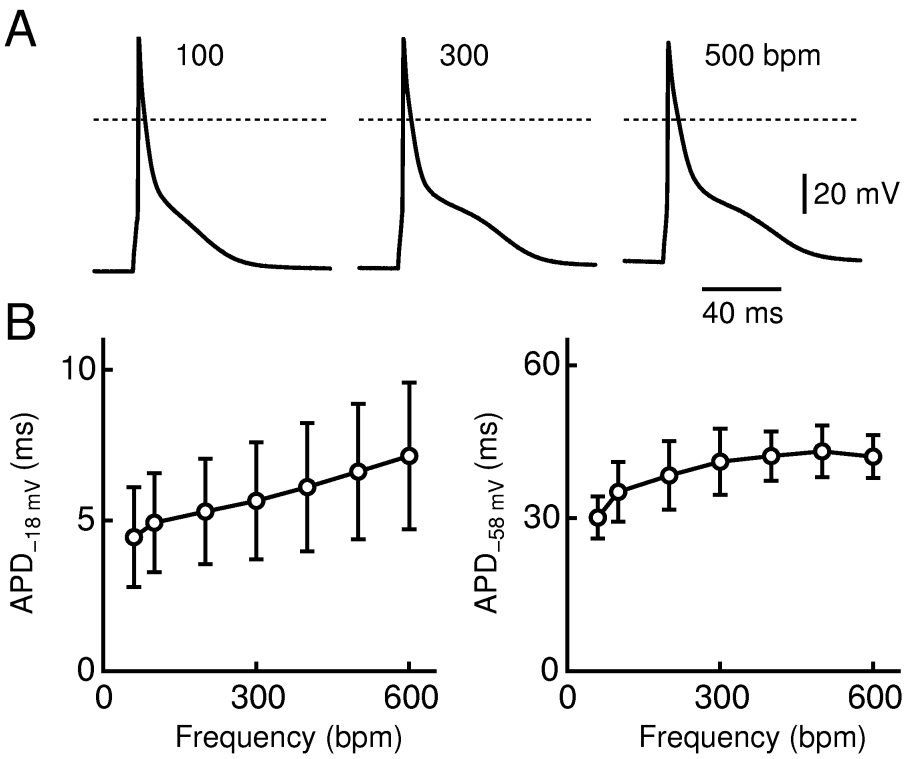

Fig. 5. Action potential of the cells. (**A**) Waveforms of the action potential recorded at a stimulation frequency of 100 (left), 300 (center), and 500 bpm (right). Dotted lines indicate 0-mV level. (**B**) Dependence of the action potential duration measured at repolarization to –18 mV (left) and at –58 mV (right) on the frequency of stimulation. Error bars indicate SD (n = 8).

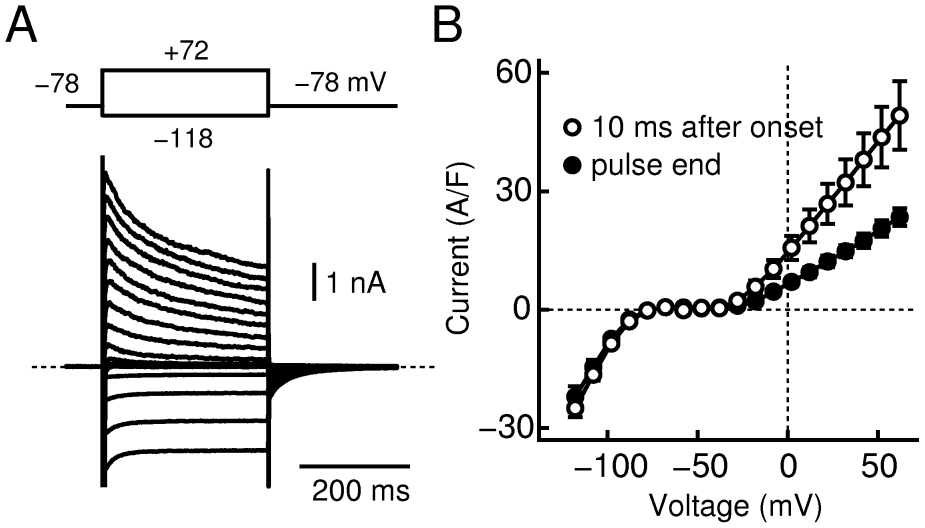

Fig. 6. Macroscopic membrane current of the cells. (**A**) A family of current records evoked by 300 ms single pulses of the voltages from –118 to +72 mV in 10 mV increments from a holding potential of –78 mV (inset). The dotted line indicates zero-current level. Membrane capacitance was 113 pF. (**B**) I-V relations of the current, measured at 10 ms after the pulse onset (open circles) and at the pulse end (solid circles). Error bars indicate SD (n = 8).

cause the intracellular Ca^{2+} was chelated with 1 mM EGTA in the pipette solution.

At a stimulation frequency of 300 bpm, the action potential peaked at +42.8 ± 2.0 mV (n = 8). Its duration at this frequency, measured at –18 mV (APD_{-18mV}, corresponding to 50% repolarization), was 5.7 ± 2.0 ms (n = 8), and at –58 mV (APD_{-58mV}, corresponding to 85% repolarization), it was 41 ± 7 ms (n = 8). The APD_{-18mV} and the APD_{-58mV} both became longer with increasing stimulation frequency (Fig. 5B), as was also reported in regard to intact mouse hearts [24].

Macroscopic membrane currents of the cells

Under the same conditions, macroscopic membrane currents were also recorded in Fig. 6. The cells were voltage-clamped at a holding potential of –78 mV, and the membrane current was evoked every 4 s with 300-ms single pulses to the voltages from –118 to +72 mV. In the current records of Fig. 6A, it is obvious that the transient outward current (I_{to}) was activated in the voltage range above –30 mV, and that the inward-rectifier K^+ current was in the range below –80 mV. Between these ranges, the current records were almost flat (except for a large inward Na^+ current that was too fast to be resolved in Fig. 6A), which was also evident in the I-V relations (Fig. 6B). This voltage dependence of the macroscopic membrane current is consistent with previous reports in mouse heart cells [11, 25].

Response of the cells to β-adrenergic stimulation

As a test for receptor-mediated signal transduction in the cells, the effect of isoproterenol to the L-type Ca^{2+} current (I_{Ca}) was examined in Fig. 7. The cells were whole-cell clamped, using the Cs^+-pipette solution, in the Cs^+-Tyrode solution at 37°C. The I_{Ca} was evoked by using a double-pulse protocol to +2 mV applied from a holding potential of –78 mV every 4 s. In the records of the I_{Ca} (Fig. 7A), the inward Na^+ current activated during the

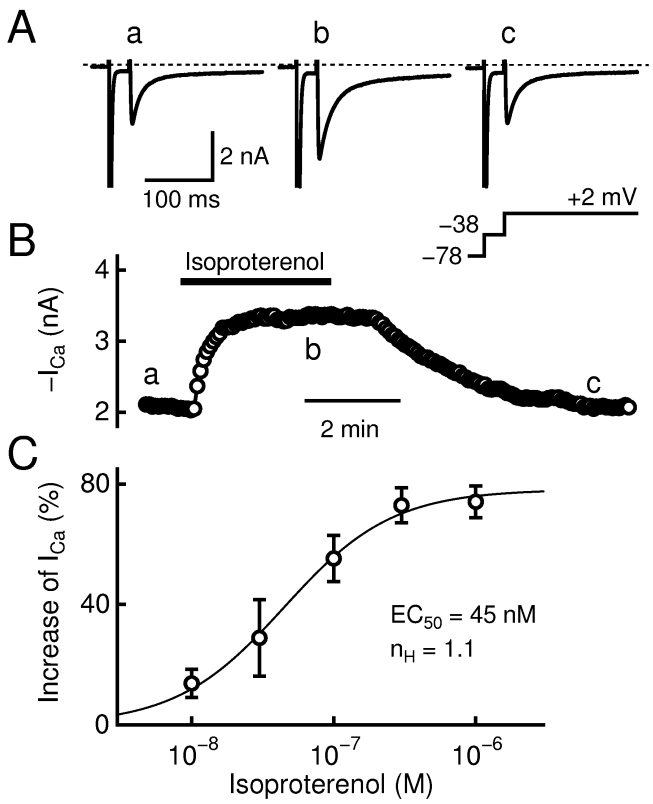

Fig. 7. Enhancement of the I_{Ca} by isoproterenol. (**A**) Records of the I_{Ca} before (**a**), during (**b**), and after (**c**) the application of isoproterenol (300 nM). The I_{Ca} was evoked using a double pulse to –38 mV for 30 ms then to +2 mV for 200 ms from a holding potential of –78 mV (inset). The dotted line indicates zero-current level. Membrane capacitance was 230 pF. (**B**) The time course of the peak I_{Ca} amplitude at +2 mV. The horizontal bar indicates the period of isoproterenol (300 nM) application. Letters (**a**–**c**) indicate the times of the records in panel A. (**C**) The dose-response relation of the I_{Ca} enhancement by isoproterenol. Data points represent the percent increase of the peak I_{Ca} amplitude relative to the control level before the application of isoproterenol. Error bars indicate SEM (n = 4–24).

prepulse was also prominent. The I_{Ca} had a peak amplitude of –10.3 ± 2.4 A/F (n = 20) at +2 mV, and the application of isoproterenol (1 μM) increased the amplitude by 77 ± 20% (n = 20) in a reversible manner (Fig. 7, A and B). The half-maximal effective concentration (EC_{50}) and Hill coefficient (n_H) of the I_{Ca} enhancement by isoproterenol in the cells were 45 nM and 1.1, respectively (Fig. 7C); these values are comparable to those reported previously [6, 7].

DISCUSSION

This report has described a novel technique that isolates healthy heart cells from mouse models. With the aid of the simple devices, this technique enabled an easy and reproducible isolation of healthy heart cells from small mouse hearts under physiological conditions. Thus isolated cells had a consistently high viability and a long storage life, as well as normal electrophysiological and contraction properties. The cells also had a normal response to β-adrenergic stimulation.

Comparison with other heart cell isolation techniques

The advantage of this technique is that it provides a reproducible method for isolating healthy heart cells. The use of the cannulation device and the aortic cannula (Figs. 1 and 2) has eliminated the issues of the handling and cannulation of small mouse hearts, making these maneuvers highly reproducible. The isolated cells had a consistently high viability of 75 ± 5%, which is comparable to the highest values (84–90%) reported so far for mouse heart cells [12, 13], and a long storage life (>8 h) under physiological conditions (Fig. 3). The reproducibility of this technique and the consistency of the cells' quality shall provide more ease and efficiency to single-cell studies of the heart using mouse models.

Another advantage of this technique is that the cells are isolated and stored under physiological conditions. Although it used insulin (50 μU/ml) and high glucose (22 mM) to stimulate glucose utilization [26], they were used only during cell isolation (~70 min) at physiological levels [27]. This is in contrast to the other methods that use "KB" medium [10, 11] or BDM [12, 13], both of which are not natural to the cells and have been reported to affect their normal physiology.

Incubating the cells in high-K^+, Ca^{2+}-free "KB" medium at 4°C is a very popular work-around for reducing cell damage [14]. Reports have shown, however, that a long exposure of heart cells to Ca^{2+}-free condition degrades their surface glycocalix, and also that it permeabilizes the sarcolemmal membrane to ions and small molecules [14, 15, 28, 29]. Alternatively, the administration of 10–20 mM BDM in the media for cell isolation is also widely used for reducing cell damage [12, 30]. However, reports have shown that BDM affects the electrophysiological and contraction properties of heart cells, as well as their Ca^{2+} signaling, via direct action, protein phosphorylation, and/or altered gene expression [16, 17, 31–33].

The yield of the cells in this method is estimated to be ~3×10^6 cells/heart. This is calculated from the volume of the cell pellet after centrifugation (~0.1 ml) and from the dimensions of the cells (157 × 25 μm), assuming a cell thickness of 8 μm. This cell yield is comparable to the value reported previously (5.3×10^5 cells/left ventricle) [13].

What affects cell quality

In this technique, several things critically affect cell quality. The first is maintaining a fast flow rate throughout the period of coronary perfusion. To ensure this, air embolism of the coronary artery was prevented by cannulating the aorta under the solution level and by using the aortic cannula that also functioned as an air trap. Making an incision in the interventricular septum was also very effective to maintain a fast flow rate.

The second is the duration of initial EGTA-CIB perfusion. A complete removal of Ca^{2+} from the coronary artery was absolutely necessary before the application of enzymes. When EGTA-CIB perfusion was too short and the Ca^{2+} removal was incomplete, the perfusion flow stopped after a switch to the enzyme solution, and this led to poor tissue digestion and very severe damages to the isolated cells. Also, many small white spots developed on the heart's surface along the coronary artery. On the other hand, when the perfusion was too long the cells were "paradoxically" damaged by the Ca^{2+}-free environment in EGTA-CIB, and they had an impaired Ca^{2+} tolerance [29] as also reported by Wolska and Solaro [17]. Although the duration of initial EGTA-CIB perfusion involves a trade-off, 3–4 min was adequate for the heart of adult mice.

The third is a thorough tissue digestion. This requires a certain level of proteolytic activity; however, that in the collagenase (CLS-2, Worthington Biochemical) is usually insufficient. Therefore in this technique, trypsin (type I, Sigma) and protease (type XIV, Sigma) were used to facilitate tissue digestion and single-cell dispersion, respectively. Because their optimal doses varied with the collagenase's lot and the mouse's age, the doses were adjusted in the range 0.03–0.12 mg/ml to achieve a thorough tissue digestion. In general, more doses were necessary for older animals and for the collagenase's lots with lower protease activity.

The fourth is the anesthesia. The dose of pentobarbital sodium was unexpectedly, but strongly influential on the cells' quality, and an insufficient dose resulted in sizable cell damage. Thus a highly overdosed amount (300 mg/kg, i.p.) was used in this technique. The effect may be attributed to the coronary-dilating action of pentobarbital [34], which would facilitate a fast perfusion of the heart. The effect might also be attributed to the action of pentobarbital to suppress catecholamine release from adrenal

chromaffin cells at a comparable level (500 μM, or 124 mg/*l*, i.v.) to that used in this technique (300 mg/kg, i.p.) [35]. This action would prevent Ca^{2+}-overloading of the cells that would be caused by an elevated plasma catecholamine level during the surgery [36].

Regarding water quality, it was not very critical in this technique. No obvious difference was found in the cells' quality between milli-Q water and regular distilled water.

Properties of the isolated heart cells

The unloaded contraction of the cells showed a negative frequency dependence (Fig. 4). This agrees with preceding reports that described a negative force-frequency relationship in single mouse heart cells [17, 19]. However, in the range of physiological heart rates (200–600 bpm, or 3.3–10 Hz), the contraction amplitude showed no detectable frequency dependence. This observation conforms with the other reports that showed the negative force-frequency relationship of mouse heart muscle, which developed only at stimulation frequencies lower than 1–2 Hz [22, 23].

The duration of the action potential's overshoot, or APD_{-18mV}, had a large variation among the cells (Fig. 5). In good agreement to this, a large variation was also observed in the I_{to} amplitudes that determine the rate of the repolarization of the overshoot (Fig. 6). The variations in the APD_{-18mV} and in the I_{to} amplitudes may indicate the regional heterogeneity of repolarizing K^+ current reported in mouse heart cells [37, 38].

The β-adrenergic stimulation by isoproterenol induced a large increase of the I_{Ca} (77 ± 20% at 1 μM, Fig. 7). Moreover, the values of the EC_{50} and Hill coefficient of this response (45 nM and 1.1, respectively) were near those reported for mouse heart cells under comparable conditions: 36 nM and 1.0 [7], and 57.1 nM and 1.0 [6]. These observations indicate that the β-adrenoceptor–mediated signal transduction system in the cells is normal and fully functional.

REFERENCES

1. Bockamp E, Maringer M, Spangenberg C, Fees S, Fraser S, Eshkind L, et al. Of mice and models: improved animal models for biomedical research. Physiol Genomics. 2002;11:115-32.
2. Santana LF, Kranias EG, Lederer WJ. Calcium sparks and excitation-contraction coupling in phospholamban-deficient mouse ventricular myocytes. J Physiol. 1997;503:21-9.
3. Nerbonne JM, Nichols CG, Schwarz TL, Escande D. Genetic manipulation of cardiac K^+ channel function in mice: what have we learned, and where do we go from here? Circ Res. 2001;89:944-56.
4. Xiao RP, Avdonin P, Zhou YY, Cheng H, Akhter SA, Eschenhagen T, et al. Coupling of β_2-adrenoceptor to G_i proteins and its physiological relevance in murine cardiac myocytes. Circ Res. 1999;84:43-52.
5. Dilly KW, Kurokawa J, Terrenoire C, Reiken S, Lederer WJ, Marks AR, Kass RS. Overexpression of β_2-adrenergic receptors cAMP-dependent protein kinase phosphorylates and modulates slow delayed rectifier potassium channels expressed in murine heart: evidence for receptor/channel co-localization. J Biol Chem. 2004;279:40778-87.
6. Sako H, Green SA, Kranias EG, Yatani A. Modulation of cardiac Ca^{2+} channels by isoproterenol studied in transgenic mice with altered SR Ca^{2+} content. Am J Physiol Cell Physiol. 1997;273:C1666-72.
7. Brittsan AG, Ginsburg KS, Chu G, Yatani A, Wolska BM, Schmidt AG, et al. Chronic SR Ca^{2+}-ATPase inhibition causes adaptive changes in cellular Ca^{2+} transport. Circ Res. 2003;92:769-76.
8. Mohler PJ, Schott JJ, Gramolini AO, Dilly KW, Guatimosim S, duBell WH, et al. Ankyrin-B mutation causes type 4 long-QT cardiac arrhythmia and sudden cardiac death. Nature. 2003;421:634-9.
9. Salama G, London B. Mouse models of long QT syndrome. J Physiol. 2007;578:43-53.
10. Benndorf K, Boldt W, Nilius B. Sodium current in single myocardial mouse cells. Pflugers Arch. 1985;404:190-6.
11. Fiset C, Clark RB, Larsen TS, Giles WR. A rapidly activating sustained K^+ current modulates repolarization and excitation-contraction coupling in adult mouse ventricle. J Physiol. 1997;504:557-63.
12. Sambrano GR, Fraser I, Han H, Ni Y, O'Connell T, Yan Z, Stull JT. Navigating the signalling network in mouse cardiac myocytes. Nature. 2002;420:712-4.
13. Zhou YY, Wang SQ, Zhu WZ, Chruscinski A, Kobilka BK, Ziman B, et al. Culture and adenoviral infection of adult mouse cardiac myocytes: methods for cellular genetic physiology. Am J Physiol Heart Circ Physiol. 2000;279:H429-36.
14. Isenberg G, Klöckner U. Calcium tolerant ventricular myocytes prepared by preincubation in a "KB" medium. Pflugers Arch. 1982;395:6-18.
15. Winegrad S. Studies of cardiac muscle with a high permeability to calcium produed by treatment with ethylenediaminetetraacetic acid. J Gen Physiol. 1971;58:71-93.
16. Sellin LC, McArdle JJ. Multiple effects of 2,3-butanedione monoxime. Pharmacol Toxicol. 1994;74:305-13.
17. Wolska BM, Solaro RJ. Method for isolation of adult mouse cardiac myocytes for studies of contraction and microfluorimetry. Am J Physiol Heart Circ Physiol. 1996;271:H1250-5.
18. Shioya T, Ehara T. A simple method for isolating single heart cells from mouse models. J Physiol Sci. 2007;57:S202.
19. Wussling M, Schenk W, Nilius B. A study of dynamic properties in isolated myocardial cells by the laser diffraction method. J Mol Cell Cardiol. 1987;19:897-907.
20. Olsson MC, Palmer BM, Stauffer BL, Leinwand LA, Moore RL. Morphological and functional alterations in ventricular myocytes from male transgenic mice with hypertrophic cardiomyopathy. Circ Res. 2004;94:201-7.
21. Wehrens XHT, Kirchhoff S, Doevendans PA. Mouse electrocardiography: an interval of thirty years. Cadiovasc Res. 2000;45:231-7.
22. Endoh M. Force-frequency relationship in intact mammalian ventricular myocardium: physiology and pathophysiological relevance. Eur J Phamacol. 2004;500:73-86.
23. Tanaka H, Namekata I, Takeda K, Kazama A, Shimizu Y, Moriwaki R, et al. Unique excitation-contraction characteristics of mouse myocardium as revealed by SEA0400, a specific inhibitor of Na^+-Ca^{2+} exchanger. Naunyn-Schmiedeberg's Arch Pharmacol. 2005;371:526-34.
24. Knollmann BC, Schober T, Petersen AO, Sirenko SG, Franz MR. Action potential characterization in intact mouse heart: steady-state cycle length dependence and electrical restitution. Am J Physiol Heart Circ Physiol. 2007;292:H614-21.
25. Knollmann B, Knollmann-Ritschel BEC, Weissman NJ, Jones LR, Morad M. Remodelling of ionic currents in hypertrophied and failing hearts of transgenic mice overexpressing calsequestrin. J Physiol. 2000;525:483-98.
26. Brownsey RW, Boone AN, Allard MF. Actions of insulin on the mammalian heart: metabolism, pathology and biochemical mechanisms. Cardiovasc Res. 1997;34:3-24.
27. Ahrén B. ANF inhibits glucose-stimulated insulin secretion in mouse and rat. Am J Physiol Endocrinol Metab. 1988;225:E579-82.
28. McClellan GB, Winegrad S. The regulation of the calcium sensitivity of the contractile system in mammalian cardiac muscle. J Gen Physiol. 1978;72:737-64.
29. Daly MJ, Elz JS, Nayler WG. Contracture and the calcium paradox in the rat heart. Circ Res. 1987;61:560-9.
30. Thum T, Borlak J. Butandione monoxime increases the viability and yield of adult cardiomyocytes in primary cultures. Cardiovasc Toxicol. 2001;1:61-72.
31. Artigas P, Al'Aref SJ, Hobart EA, Díaz LF, Sakaguchi M, Straw S, et al. 2,3-butanedione monoxime affects cystic fibrosis transmembrane conductance regulator channel function through phosphorylation-dependent and phosphorylation-independent mechanisms: the role of bilayer material properties. Mol Pharmacol. 2006;70:2015-26.
32. Watanabe Y, Iwamoto T, Matsuoka I, Ohkubo S, Ono T, Watano T, et al. Inhibitory effect of 2,3-butanedione monoxime (BDM) on Na^+/Ca^{2+} exchange current in

guinea-pig cardiac ventricular myocytes. Br J Phamacol. 2001;132:1317-25.
33. Borlak J, Zwadlo C. The myosin ATPase inhibitor 2,3-butanedione monoxime dictates transcriptional activation of ion channels and Ca^{2+}-handling proteins. Mol Pharmacol. 2004;66:708-17.
34. Manders WT, Vatner SF. Effects of sodium pentobarbital anesthesia on left ventricular function and distribution of cardiac output in dogs, with particular reference to the mechanism for tachycardia. Circ Res. 1976;39:512-7.
35. Pocock G, Richards CD. The action of pentobarbitone on stimulus-secretion coupling in adrenal chromaffin cells. Br J Pharmacol. 1987;90:71-80.
36. Cryer PE. Physiology and pathophysiology of the human sympathoadrenal neuroendocrine system. N Engl J Med. 1980;303:436-44.
37. Guo W, Xu H, London B, Nerbonne JM. Molecular basis of transient outward K^+ current diversity in mouse ventricular myocytes. J Physiol. 1999;521:587-99.
38. Brunet S, Aimond F, Li H, Guo W, Eldstrom J, Fedida D, et al. Heterogeneous expression of repolarizing, voltage-gated K^+ currents in adult mouse ventricles. J Physiol. 2004;559:103-20.